

# Deep Learning Towards Edge Computing: Neural Networks Straight from Compressed Data

Samuel Felipe dos Santos, Jurandy Almeida

*Instituto de Ciência e Tecnologia, Universidade Federal de São Paulo – UNIFESP  
12247-014, São José dos Campos, SP – Brazil*

---

## Abstract

Due to the popularization and grow in computational power of mobile phones, as well as advances in artificial intelligence, many intelligent applications have been developed, meaningfully enriching people's life. For this reason, there is a growing interest in the area of edge intelligence, that aims to push the computation of data to the edges of the network, in order to make those applications more efficient and secure.

Many intelligent applications rely on deep learning models, like convolutional neural networks (CNNs). Over the past decade, they have achieved state-of-the-art performance in many computer vision tasks. To increase the performance of these methods, the trend has been to use increasingly deeper architectures and with more parameters, leading to a high computational cost. Indeed, this is one of the main problems faced by deep architectures, limiting their applicability in domains with limited computational resources, like edge devices.

To alleviate the computational complexity, we propose a deep neural network capable of learning straight from the relevant information pertaining to visual content readily available in the compressed representation used for image and video storage and transmission. The novelty of our approach is that it was designed to operate directly on frequency domain data, learning with DCT coefficients rather than RGB pixels. This enables to save high computational load in full decoding the data stream and therefore greatly speed up the processing time, which has become a big bottleneck of deep learning.

We evaluated our network on two challenging tasks: (1) image classification on the ImageNet dataset and (2) video classification on the UCF-101 and HMDB-51 datasets. Our results demonstrate comparable effectiveness to the state-of-the-art methods in terms of accuracy, with the advantage of being more computationally efficient.

**Keywords:** Edge Intelligence, Deep Learning, Convolutional Neural Network, Computational Efficiency, Compressed-Domain Processing

---

*Email addresses:* felipe.samuel@unifesp.br (Samuel Felipe dos Santos),  
jurandy.almeida@unifesp.br (Jurandy Almeida)

---

## 1. Introduction

Convolutional neural networks (CNNs) have brought astonishing advances in computer vision, being used in several application domains, such as medical imaging, autonomous driving, road surveillance, and many others [1, 2]. However, in order to increase the performance of these methods, increasingly deeper architectures have been used, leading to models with higher computational costs and larger number of parameters [3]. To accelerate this compute-intensive workload, it is required specialized hardware accelerators and optimized data flows, making it impossible to be available anytime and anywhere for end users [4, 5].

Intelligent applications, like intelligent personal assistants, personalized shopping recommendation, video surveillance, and smart home appliances have gained a lot o popularity recently due to the advances made in artificial intelligence, and are able to meaningfully enrich people’s life [6]. But even though edge devices computational power have been increasing, it still not enough to support some deep learning-based applications, like voice assistants, demanding the use of cloud-based computing and, for this reason, it would not work without network connection [5].

On cloud computing, the data need to be moved from the user device to a central data center, but according to Cisco’s forecast [7], by 2021, mobile users will have generated 850 ZB of data that need to be uploaded to cloud service [5]. Moving this big amounts of data from edge devices to data center for processing can create problems like high transmission delays and risk of privacy leakage [6].

Edge computing has emerged as an alternative to overcome this problems, with the goal of pushing the cloud services from the core of the network to its edges [6]. The combination of edge computing and artificial intelligence leaded to the creation of a new paradigm called edge intelligence, or mobile intelligence, that aims to collect, cache, process, and analyze data in a network of devices in close proximity of each other, enhancing the quality, speed and security of data processing [5].

In spite of all the advances, the computational cost is still one of the main problems faced by deep learning architectures [8]. The need for high processing power and abundant memory capacity makes it difficult to apply such models to devices whose available computing resources are limited, like mobile phones and other edge devices. Therefore, specialized optimizations at both software and hardware levels are an imperative need for developing efficient and effective deep learning-based solutions [4].

For storage and transmission purposes, most image and video data available are often stored in a compressed format, like JPEG, PNG and GIF for images or MPEG-4 and H.264 for videos [1]. To use this data with a typical CNN, it would be required to decode it to obtain the RGB images used as input, a task demanding high memory and computational cost [1]. A possible alternative to alleviate this problem is to design CNNs capable of learning with DCT coefficients rather than RGB pixels [1, 8, 9, 10, 11, 12]. This information can be

easily extracted by partial decoding the data stream and fed it to the network, saving computational cost.

In this paper, we evaluated the potential of CNNs designed for the compressed domain. For this study, we consider a state-of-the-art CNN recently proposed by Gueguen et al. [9], which is a modified version of the ResNet-50 architecture [13]. Despite the speed-up obtained by partially decoding compressed data, the changes introduced by Gueguen et al. [9] in the ResNet-50 lead to a significant decrease in its computational efficiency. To alleviate its computational complexity and number of parameters, we extended the modified ResNet-50 network of Gueguen et al. [9] to include a Frequency Band Selection (FBS) technique for selecting the most relevant DCT coefficients before feeding them to the network.

Extensive experiments were conducted on two challenging tasks: (1) image classification on the ImageNet dataset and (2) video classification on the UCF-101 and HMDB-51 datasets. Our experiments analyzed the impact on computational complexity and accuracy of our network when only the 64, 32, and 16 lowest frequency DCT coefficients of each color component were used as input. We also evaluated the performance of our network for classification tasks with different difficulty levels and under different spatial resolutions and quality settings. The reported results indicate that our network can provide comparable or superior effectiveness to existing baselines, but it is much more efficient, since it has the lowest computational complexity and is the fastest for performing inferences.

A preliminary version of this work was presented at ICIP 2020 [14]. Here, we redesign our network for processing compressed videos in addition to compressed images. Also, new experiments were performed both for the analysis of our network and for the comparison with other techniques. The new reported results show the potential of our network for handling compressed domain information.

The remainder of this paper is organized as follows. Section 2 briefly reviews image and video compression algorithms. Section 3 discusses related work. Section 4 describes our approach to reduce the computational cost for decoding images and videos by training CNNs directly on the compressed data. Section 5 presents the experimental setup and reports our results. Finally, we offer our conclusions and directions for future work in Section 6.

## 2. Image and Video Compression

Compression of image and video data aims to minimize the spatial and temporal redundancies by exploiting image transforms and motion compensation, respectively [15]. Therefore, a lot of superfluous information can be discarded by processing compressed data. This section presents a brief overview about JPEG and MPEG compression.

### 2.1. Review of JPEG

The JPEG standard (ISO/IEC 10918) was created in 1992 and is currently the most widely-used image coding technology for lossy compression of digital

images. The basic steps of the JPEG compression algorithm are presented in Figure 1.

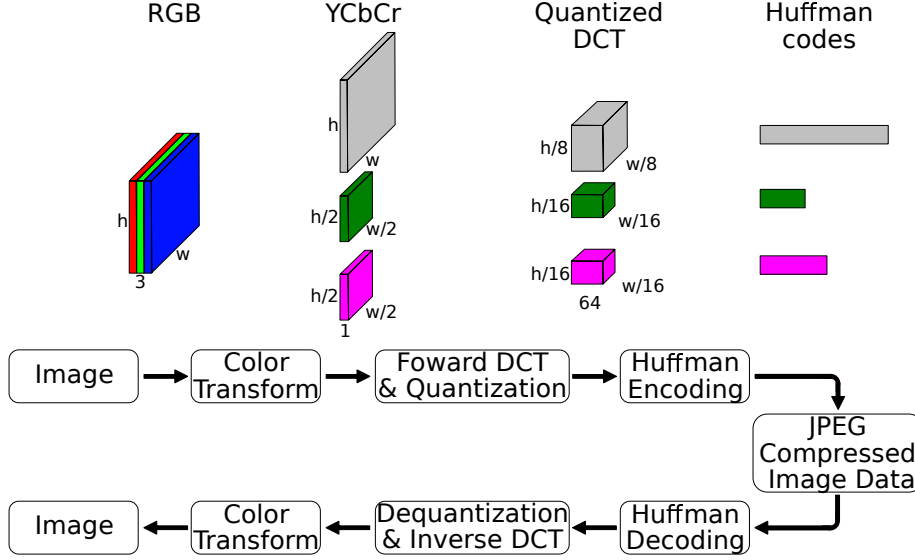


Figure 1: JPEG compression and decompression process [9].

Initially, the representation of the colors in the image is converted from RGB to YCbCr, which is composed of one luminance component (Y), representing the brightness, and two chrominance components, Cb and Cr, representing the color. Also, the Cb and Cr components are down-sampled horizontally and vertically by a factor of 2, as human vision is more sensitive to brightness details than to color details. Then, each of the three components is partitioned into blocks of 8x8 pixels and 128 is subtracted from all the pixel values. Next, each block is converted to a frequency domain representation by the forward discrete cosine transform (DCT). The result is an 8x8 block of frequency coefficient values, each corresponding to the respective DCT basis functions, with the zero-frequency coefficient (DC term) in the upper left and increasing in frequency to the right and down. The amplitudes of the frequency coefficients are quantized by dividing each coefficient by a respective quantization value defined in quantization tables, followed by rounding the result to the nearest integer. High-frequency coefficients are approximated more coarsely than low-frequency coefficients, as human vision is fairly good at seeing small variations in color or brightness over large areas, but fails to distinguish the exact strength of high-frequency brightness variations. The quality setting of the encoder affects the extent to which the resolution of each frequency component is reduced. If an excessively low-quality setting is used, most high-frequency coefficients are reduced to zero and thus discarded altogether. To improve the compression ratio, the quantized blocks are arranged into a zig-zag order and then coded by the run-length encoding (RLE) algorithm. Finally, the resulting data for all 8x8

blocks are further compressed with a lossless algorithm, a variant of Huffman encoding. For decompression, inverse transforms of the same steps are applied in reverse order. If the DCT computation is performed with sufficiently high precision, quantization and subsampling are the only lossy operations whereas the others are lossless, therefore they are reversible.

## 2.2. Review of MPEG-1/2/4

MPEG videos are composed by three main types of pictures: intra-coded (I-frames), predicted (P-frames), and bidirectionally predicted (B-frames). In a video stream, such pictures are organized into sequences of groups of pictures (GOPs) [16].

A GOP must start with an I-frame and can be followed by any number of I and P-frames, which are also known as anchor frames. Several B-frames may appear between each pair of consecutive anchor frames [16].

Each video frame is divided into a sequence of non-overlapping macroblocks. For a video coded in 4:2:0 format, each macroblock consists of six 8x8 pixel blocks: four luminance (Y) blocks and two chrominance (CbCr) blocks. Each macroblock is then either intra- or inter-coded [16].

An I-frame is completely intra-coded: every 8x8 pixel block in the macroblock is transformed to the frequency domain using the discrete cosine transformation (DCT). The 64 DCT coefficients are then quantized (lossy) and entropy (run length and Huffman, lossless) encoded to achieve compression [16].

Each P-frame is predictively encoded with reference to its previous anchor frame (the previous I or P-frame). For each macroblock in the P-frame, a local region in the anchor frame is searched for a good match in terms of the difference in intensity. If a good match is found, the macroblock is represented by a motion vector to the position of the match together with the DCT encoding of the difference (or residue) between the macroblock and its match. The DCT coefficients of the residue are quantized and encoded while the motion vector is differentiated and entropy coded (Huffman) with respect to its neighboring motion vector. This is usually known as encoding with forward motion compensation. Macroblocks encoded by such a process are called as inter-coded macroblocks [16].

In order to achieve further compression, B-frames are bidirectionally predictively encoded using forward and/or backward motion compensation with reference to its nearest past and/or future I and/or P-frames [16].

The frame number, frame encoding type (I, P or B), the positions and motion vectors of inter-coded macroblocks, the number of intra-coded blocks, and the DC coefficients of each DCT encoded pixel block can be obtained by parsing and entropy (Huffman) decoding video streams. These operations take less than 20% of the computational load in the full video decoding process [17].

## 3. Related Work

The processing of compressed data has been widely-explored by many conventional image and video processing techniques as an alternative to speed up

the computation performance in a variety of applications, such as face recognition [18], image indexing and retrieval [19], video copy detection [20], and many others.

In the deep learning era, the potential of the JPEG compressed domain for neural networks has received limited attention and a few works have emerged only recently. The key idea exploited by such works consists in adapting traditional CNN architectures to facilitate the learning with DCT coefficients rather than RGB pixels.

To accelerate the training and inference speed, Gueguen et al. [9] proposed different architectural modifications to apply to the ResNet-50 network [13] in order to accommodate DCT coefficients from JPEG images and operate directly in the frequency domain. These coefficients can be obtained by partial decoding, thus saving the high computational load and memory usage in full decoding the JPEG images. Similarly, Deguerre et al. [1] proposed a fast object detection method which takes advantage of the JPEG compressed domain. For this, the Single Shot MultiBox Detector (SSD) [21] architecture was adapted to accommodate block-wise DCT coefficients as input. To preserve the spatial information of the original image, the first three blocks of the SSD network were replaced by a convolutional layer with a filter size of 8x8 and a stride of 8. In this way, each 8x8 block from JPEG compressed data is mapped into a single position in the feature maps used as input for the next layer.

In a different direction, Ehrlich and Davis [8] reformulated the ResNet architecture to perform its operations directly on the JPEG compressed domain. Since the lossless operations used by the JPEG compression algorithm are linear, they can be composed along with other linear operations and then applied to the network weights. In this way, the basic operations used in the ResNet architecture, like convolution, batch normalization, etc, were adapted to operate in the JPEG compressed domain. For the ReLU activation, which is non-linear, an approximation function was developed.

The processing of MPEG compressed videos by deep learning methods is quite recent and has been exploited only by very few works. In most of them, a video is parsed frame by frame with CNNs designed for images.

The pioneering work of Zhang et al. [10, 11] extended the two-stream architecture of Simonyan and Zisserman [22] to use motion vectors instead of optical flow maps in the temporal stream network. However, videos still need to be decoded, since the spatial stream network is fed with RGB images [16].

The recent work of Wu et al. [12] introduced a method named Compressed Video Action Recognition (CoViAR), which extends the Temporal Segment Networks (TSN) of Wang et al. [23] to work with video data in compressed form. For that, RGB images obtained by decoding I-frames and motion features computed from P-frames are provided as input to a multi-stream CNN, with one stream for each input, which are trained separately and then combined by a simple weighted average of their output scores [16]. Although this approach is efficient, it requires to decode the frequency domain representation (i.e., DCT coefficients) from I-frames to the spatial domain (i.e., RGB pixel values).

#### 4. Learning from the Compressed Domain

The DCT computation of a  $8 \times 8$  pixel block requires 1920 floating point operations (FLOPs) [24]. Although it seems negligible, computer vision tasks usually involve the processing of a great amount of images, each one containing many pixel blocks, therefore the total computational cost may be significant. Roughly speaking, DCT is a convolution with a specific filter size of  $8 \times 8$ , stride of  $8 \times 8$ , one input channel, 64 output channels, and specific, non-learned orthonormal filters. As both the filter size and stride are equal to 8, spatial information of adjacent blocks do not overlap. In theory, a standard convolutional layer may learn to behave like a DCT, but in practice, this is not trivial, as the learned bases may be undercomplete, complete but not orthogonal, or overcomplete. In spite of that, the use of DCT weights as input for a CNN is feasible, since they can be seen as the outputs of a convolution layer with frozen weights initialized from the DCT filters [9].

Motivated by the aforesaid observations, we examine ways of integrating frequency domain information into CNNs. To present date, little work has been done to exploit the DCT representation widely used in compressed data as input for neural networks [9].

The starting point for our proposal was the modified version of the ResNet-50 architecture [13] presented by Gueguen et al. [9], which is adapted to facilitate the learning with DCT coefficients rather than RGB pixels. For this, DCT coefficients obtained from the Cb and Cr components are upsampled in order to match the resolution of the Y component. Then, the three components are concatenated channel-wise, passed through a batch normalization layer, and fed to the convolution block of the second stage of the ResNet-50 network. The second and third stages of the ResNet-50 network were changed to accommodate the amount of input channels and to ensure that the number of output channels at the end of these stages is the same of the original ResNet-50 network. Due to the smaller spatial resolution of the DCT inputs, early blocks of the second stage of the ResNet-50 network were altered to have a smoother increase of their receptive fields and, for this reason, their strides were decreased in order to mimic the increase in size of the receptive fields in the original ResNet-50 network.

These changes in the ResNet-50 network raised its computation complexity and number of parameters. In this way, the speed-up obtained by partially decoding the images is outweighed by the increase in the computational cost for passing them through the network once they are loaded in memory. Motivated by the above observations, we examine different ways of dealing with those issues in the ResNet-50 network proposed by Gueguen et al. [9]. To alleviate the computational complexity and the number of parameters, we use a Frequency Band Selection (FBS) technique to select the most relevant DCT coefficients before feeding them to the network. Since higher frequency information has little visual effect on the image, we retain the  $n$  lowest frequency coefficients and analyze how they impact the accuracy of the network.

For that, the second stage of the ResNet-50 network was changed to accom-

modate the amount of retained coefficients, i.e.,  $3n$  input channels. In this way, when FBS is set to  $n = 64$ , the network architecture is the same of that proposed by Gueguen et al. [9] and the number of output channels at the end of the second stage is equals to 256, while for  $n = 16$ , it is the same amount of the original ResNet network [13], i.e., 64. A comparison among the original ResNet-50 network [13], the modified ResNet-50 network proposed by Gueguen et al. [9], and our improved version with FBS is presented in Figure 2.

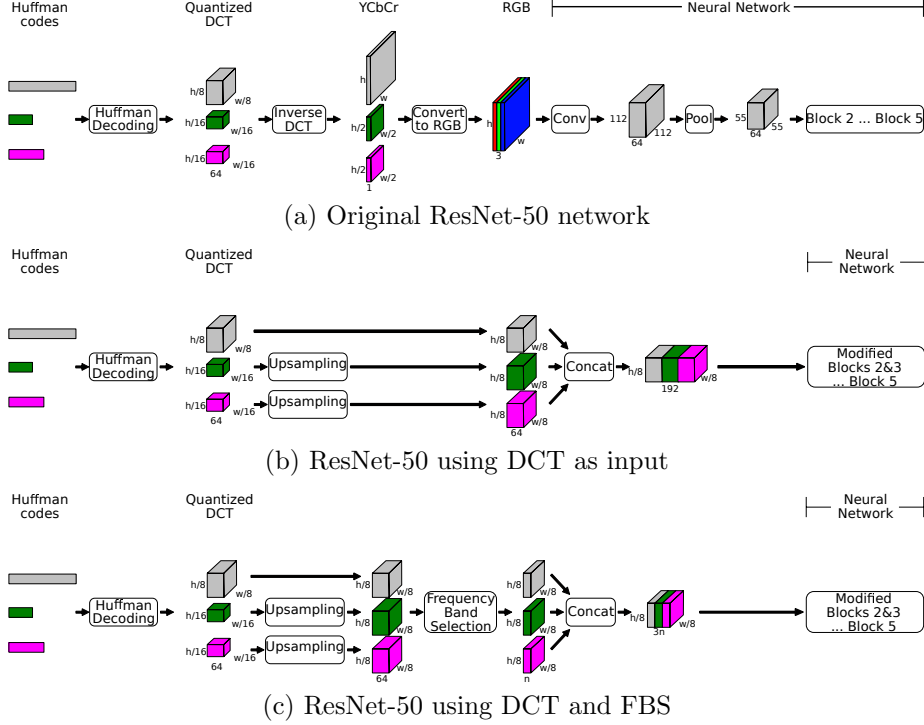


Figure 2: Illustrations of (a) the original ResNet-50 network [13], (b) the modified ResNet-50 network proposed by Gueguen et al. [9], and (c) our improved version with FBS, which selects the most relevant DCT coefficients.

We also propose an approach for using DCT coefficients in the video classification task by extending the CoViAR [12] approach to use our modified version of the ResNet-50 network [13] fed with DCT coefficients selected by the FBS technique.

In essence, CoViAR extends TSN [23] to exploit three information available in MPEG-4 compressed streams: (1) RGB images encoded in I-frames, (2) motion vectors, and (3) residuals encoded in P-frames. Architecturally, CoViAR is a multi-stream network composed of three independent CNNs, one for each of these three information. Similar to TSN [23], CoViAR models long-range temporal dynamics by learning from multiple segments of a video. For this,



uniform sampling is used to take a set of frames. Then, frame scores are obtained by feeding the network with one frame at a time. Next, a video score is obtained by averaging the frame scores. Finally, late fusion is performed to take a final prediction, which is computed by the weighted average of the video scores from all the three streams.

Although CoViAR has been designed to operate with video data in the compressed domain, it still demands a preliminary decoding step, since the frequency domain representation (i.e., DCT coefficients) used to encode the pictures in I-frames and the residuals in P-frames needs to be decoded to the spatial domain (i.e., RGB pixel values) before being fed to the network. In fact, CoViAR relies on CNNs designed for processing RGB images, which are not able to learn directly from frequency domain data.

Roughly speaking, our approach for video classification extends CoViAR to take advantage of the modified ResNet-50 network with FBS we proposed, enabling it to operate directly on the frequency domain, speeding up the processing time. For this reason, we named our approach as Fast-CoViAR (Fast Compressed Video Action Recognition). The similarities and differences of CoViAR and Fast-CoViAR can be observed in Figure 3. Architecture wise, Fast-CoViAR is a two-stream network which employs two different CNNs as the front-end to learn the frequency and temporal information of a compressed video, respectively. Unlike CoViAR, instead of a spatial stream using the ResNet-152 network and RGB pixels as input, the frequency stream corresponds to the modified ResNet-50 network with FBS and is fed with DCT coefficients from I-frames. Similar to CoViAR, the temporal stream is implemented by a ResNet-18 network fed with motion vectors from P-frames. Different from CoViAR, we choose not to include a stream for processing residuals from P-frames, once it only results in a slight increase of performance (i.e., gains less than 0.5%) at the cost of a significant increase in computational complexity.

The learning procedure of Fast-CoViAR is performed as follows. Initially, a compressed video is parsed and a set of encoded frames for each stream is obtained by uniform sampling. Then, encoded frames are entropy decoded and passed through the network, one frame at a time, generating frame scores. Next, frame scores of each stream are averaged to produce a video score. Finally, the final prediction is obtained by a simple late fusion, which consists of a weighted average between the video score of both streams.

## 5. Experiments and Results

This section presents the experimental protocol and the results obtained by our network. Section 5.1 presents the experiments on image classification performed with our modified ResNet-50 using DCT and FBS, and Section 5.2 reports the results for video classification obtained by our proposed Fast-CoViAR.

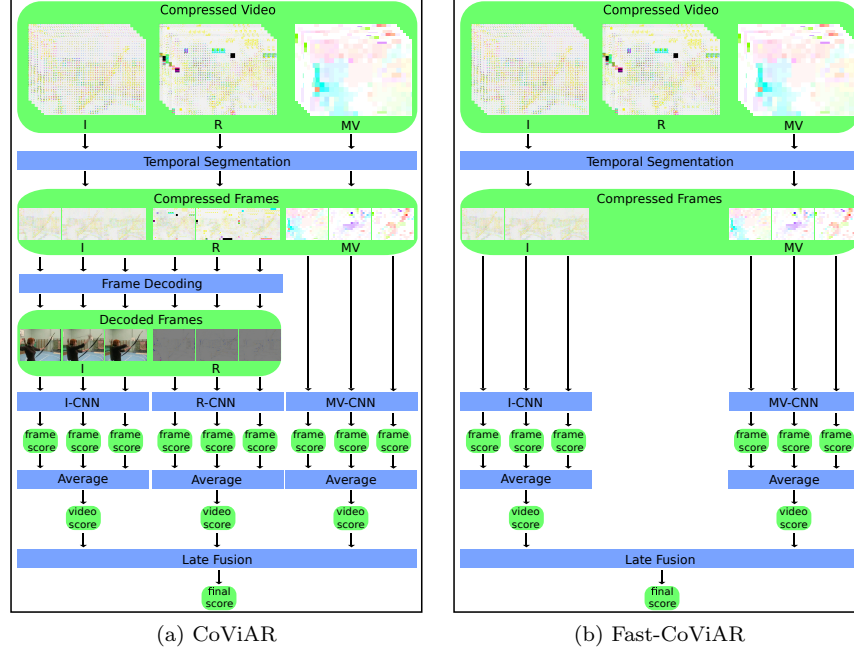


Figure 3: Illustrations of (a) the CoViAR [12] method, and (b) our proposed Fast-CoViAR. Unlike CoViAR, where I-frames need to be decoded before being fed to the network, Fast-CoViAR is designed to operate directly on frequency domain data, learning with DCT coefficients rather than RGB pixels.

### 5.1. Image Classification

Our first experiments were conducted on a subset of the ImageNet [25] dataset<sup>1</sup>. For that, 211 of the 1000 classes were taken from the ILSVRC12 dataset and then grouped into 12 classes, namely: ball, bear, bike, bird, bottle, cat, dog, fish, fruit, turtle, vehicle, sign. This subset is composed of 268,773 images and was split into a training set of 215,018 (80%) images and a test set of 53,755 (20%) images. All the images were resized so the smallest side is 256 and the crop size is 224x224. These experiments are intend to evaluate the impact of image resolution, JPEG image quality, and classification tasks with different difficulty levels: fine-grained, where 211 out of 1000 classes from the ILSVRC12 dataset were used, and coarse-grained, where these classes are grouped into 12 categories. After that, we evaluated the classification accuracy of our network on the entire ImageNet dataset.

All the experiments were performed using the ResNet-50 architecture, batch

<sup>1</sup>The script for generating the ImageNet subset is available at <https://github.com/dusty-nv/jetson-inference/blob/master/tools/imagenet-subset.sh> (As of October, 2020)

size of 128, initial learning rate of 0.05, momentum of 0.9, and were trained for 120 epochs, reducing the learning rate by a factor of 10 every 30 epochs. Data augmentation with random crop and horizontal flip was used on the training phase, while on test, only a center crop was used. They were executed on a machine equipped with a processor Intel Core i7 6850K 3.6 GHz, 64 GBytes of DDR4-memory, and 3 NVIDIA Titan Xp GPUs. The machine runs Ubuntu 18.04 LTS (kernel 5.0.0) and the ext4 file system.

Note that the network proposed by Gueguen et al. [9] (ResNet-50 + DCT) has a higher computational complexity than the original ResNet-50 [13] (ResNet-50 + RGB). This is due to the increase in the number of channels and receptive field size of the second and third stages of the network. Our FBS (ResNet-50 + DCT + FBS) reduced the computational complexity and the number of parameters with respect to the network of Gueguen et al. [9]. By using 16 DCT coefficients for each color component, our network is faster than the original ResNet-50 and has the same amount of parameters.

Table 1 compares the accuracy of the original ResNet-50 network and its modified versions for image classification tasks with different difficulty levels. The value inside parentheses is the number of input channels of each network.

Table 1: Comparison of accuracy (%) for the original ResNet-50 with RGB inputs and networks using DCT as input for image classification tasks with different difficulty levels.

Approach	Classification Task	
	<i>Fine</i> (211 Classes)	<i>Coarse</i> (12 Classes)
ResNet-50 + RGB (3x1) [13]	76.28	96.49
ResNet-50 + DCT (3x64) [9]	70.28	94.15
ResNet-50 + DCT + FBS (3x32)	69.79	94.53
ResNet-50 + DCT + FBS (3x16)	68.12	93.92

For both tasks, the RGB-based network (ResNet-50 + RGB) performed better than the DCT-based ones. In the fine-grained task, the second best network was the one proposed by Gueguen et al. [9] (ResNet-50 + DCT), which obtained a result 6% less than the RGB. In the coarse-grained task, the second best result was achieved by the network fed with 32 DCT coefficients per color component selected by our FBS (ResNet-50 + DCT + FBS), whose accuracy is only 1.96% lower than the RGB. In both tasks, the accuracy between the DCT-based networks were similar and, in the coarse-grained task, the use of our FBS with 32 DCT coefficients yielded better results than the network of Gueguen et al. [9].

Table 2 compares the accuracy of the original ResNet-50 network and its modified versions for image classification with different spatial resolution. For this, we resized all the images to have their smallest side with 256, 128, 64, and 32 pixels and used the crop sizes of 224x224, 112x112, 56x56, and 28x28, respectively. As it can be seen, the reduction in the spatial resolution yielded a significant impact on the performance of all the networks, although the DCT-based ones were more affected, significantly reducing the accuracy.

Table 2: Comparison of accuracy (%) for the original ResNet-50 with RGB inputs and networks using DCT as input for images with different resolutions.

Approach	Image Resolution			
	<i>32</i>	<i>64</i>	<i>128</i>	<i>256</i>
ResNet-50 + RGB (3x1) [13]	81.82	90.39	94.56	96.49
ResNet-50 + DCT (3x64) [9]	72.72	82.06	90.32	94.15
ResNet-50 + DCT + FBS (3x32)	71.83	82.22	90.78	94.53
ResNet-50 + DCT + FBS (3x16)	70.35	81.35	90.16	93.92

We also analyzed the effect of reducing the quality setting used to encode JPEG images, as can be observed in Table 3. All the networks were robust to this parameter, yielding a small drop in accuracy, lower than 1% even for the worse quality setting.

Table 3: Comparison of accuracy (%) for the original ResNet-50 with RGB inputs and networks using DCT as input for images with different JPEG qualities.

Approach	JPEG Quality			
	<i>25</i>	<i>50</i>	<i>75</i>	<i>100</i>
ResNet-50 + RGB (3x1) [13]	95.78	95.98	96.09	96.49
ResNet-50 + DCT (3x64) [9]	93.84	94.02	94.50	94.15
ResNet-50 + DCT + FBS (3x32)	93.63	93.97	94.20	94.53
ResNet-50 + DCT + FBS (3x16)	92.69	93.26	93.66	93.92

Our last experiment evaluated the classification accuracy of our network on the entire ImageNet dataset, as it can be seen in Table 4. The accuracy obtained by the RGB-based network (ResNet-50 + RGB) was higher than the the DCT-based ones, similar to what was observed on the experiments with the subset. The second best result was obtained by the network proposed by Gueguen et al. [9](ResNet-50 + DCT), obtaining an accuracy 1.13% lower than the RGB. The network fed with 32 DCT coefficients per color component selected by our FBS (ResNet-50 + DCT + FBS), obtained accuracy only 3.24% lower than the RGB, while the use of 16 DCT coefficients per color component led to a greater loss in accuracy of 6.43%.

Table 4: Comparison of accuracy for the original ResNet-50 with RGB inputs and best networks using DCT as input for image classification on the ImageNet dataset.

Approach	Accuracy
ResNet-50 RGB (3x1) [13]	73.46
ResNet-50 DCT (3x64) [9]	72.33
ResNet-50 DCT + FBS (3x32)	70.22
ResNet-50 DCT + FBS (3x16)	67.03

## 5.2. Video Classification

To assess the performance of our network for video classification, we conducted experiments on two public datasets proposed for human action recognition tasks, UCF-101 and HMDB-51, each one containing a large and varied repertoire of different actions [26]. We focused on this task and chose these datasets because they are well-studied by the computer vision community, allowing us to compare our results with other works, including the approach we used as a starting point to ours, the CoViAR [12] model. However, our approach can also be applied to other video classification tasks.

The UCF-101 dataset<sup>2</sup> [27] contains 13,320 videos (27 hours) collected from YouTube. All videos are in MPEG-4 format (at 25 frames per second and 320×240 resolution), in color and with sound. They are categorized into 101 action classes and their duration varies from 1.06 to 71.04 seconds. Each of the action classes is divided into 25 groups containing 4-7 videos with common features, like actors and background. Those videos have large variations in camera motion, object appearance and pose, illumination conditions, etc.

The HMDB-51 dataset<sup>3</sup> [28] is composed of 6,766 videos (6 hours) collected from various sources, such as movies and internet sites like YouTube and Google. All videos are in MPEG-4 format (at 30 frames per second and with a fixed height of 240 pixels and width ranging from 176 to 592 pixels), in color and no sound. They are distributed among 51 action classes with at least 102 videos in each and their duration varies from 0.64 to 35.44 seconds. Such videos were annotated with information about camera motion, camera viewpoint, video quality, number of actors, visible body parts, etc.

For evaluation, three training and testing splits are provided with the UCF-101 and HMDB-51 datasets. In our experiments, we follow the official evaluation protocol, which consists in evaluating the default training and testing splits separately and reporting the average accuracy over these three splits.

Two data augmentation strategies were applied during training phase: (1) horizontal flipping with 50% probability and (2) random cropping with scale jittering. This latter consists of a cropping area whose size is selected at random from different scales (4 scales for the frequency stream: 1, 0.875, 0.75, and 0.66; and 3 scales for the temporal stream: 1, 0.875, and 0.75) and then resized to match the input size requirements of the network (i.e., 28×28 pixels for the frequency stream and 224×224 pixels for the temporal stream).

For training each stream, we follow CoViAR [12] and uniformly sample 3 frames from each video to feed the network. During testing phase, the action category is predicted by taking a uniform sample of 25 frames, each with 5 crops and horizontal flips, totaling 250 frames per video, which are passed through the network independently, with the final prediction being an average of all frame scores.

---

<sup>2</sup><http://csrcv.ucf.edu/data/UCF101.php> (As of October 2020)

<sup>3</sup><http://serre-lab.clps.brown.edu/resource/hmdb-a-large-human-motion-database/> (As of October 2020)

The ResNet models of both streams were pre-trained on the ImageNet [25] dataset and fine-tuned using Adam [29] with a batch size of 40. Step-decay was used to reduce the initial learning rate by a factor of 10 after a number of epochs. The initial learning rates, the total number of epochs, and the step-decay scheduler setting are presented in Table 5.

Table 5: The hyperparameters used for training the Fast-CoViAR network.

Hyperparameter	UCF-101		HMDB-51	
	I	MV	I	MV
<i>Initial learning rate</i>	0.00015	0.005	0.0003	0.0025
<i>Total number of epochs</i>	510		220	360
<i>The step-decay scheduler setting</i>	150, 270, 390		55, 110, 165	120, 200, 280

Table 6: Classification accuracy (%) achieved by Fast-CoViAR in the three splits of the UCF-101 and HMDB-51 datasets. In the frequency stream, ResNet-50 was used for processing DCT coefficients from I-frames; whereas ResNet-18 was used for processing motion vectors from P-frames in the temporal stream. Three versions of ResNet-50 with different input depths were tested for the frequency stream. We compare the performance of each model in isolation and also their late fusion (+) by a weighted average of their output scores. The best and the second best results are highlighted in bold and underlining, respectively.

Dataset	Picture Type	Network Architecture	Input Data	Accuracy			
				Split1	Split2	Split3	Average
UCF-101	P	ResNet-18	MV	67.6	68.9	70.9	69.1
	I	ResNet-50	DCT	78.8	80.8	80.6	80.0
			DCT w/ FBS (32)	80.9	80.7	80.4	80.7
			DCT w/ FBS (16)	78.9	76.7	78.3	78.0
	I+P	ResNet-18	MV + DCT	84.7	85.6	<b>86.6</b>	85.7
		+	MV + DCT w/ FBS (32)	<b>85.5</b>	<b>85.9</b>	86.4	<b>86.0</b>
		ResNet-50	MV + DCT w/ FBS (16)	<u>85.0</u>	83.9	85.1	84.7
HMDB-51	P	ResNet-18	MV	38.5	37.3	40.4	38.7
	I	ResNet-50	DCT	47.8	44.6	42.4	45.0
			DCT w/ FBS (32)	45.9	43.6	41.9	43.8
			DCT w/ FBS (16)	46.6	42.2	40.6	43.1
	I+P	ResNet-18	MV + DCT	<b>56.1</b>	<b>52.3</b>	<b>51.3</b>	<b>53.3</b>
		+	MV + DCT w/ FBS (32)	55.8	51.5	50.9	52.7
		ResNet-50	MV + DCT w/ FBS (16)	55.7	50.4	50.3	52.1

Three different versions of the ResNet-50 network were tested for processing I-frames in the frequency stream: the modified version of Gueguen et al. [9], which has an input depth of 64 DCT coefficients for each color channel and is referred as DCT; and its two improved versions proposed we proposed, denoted as DCT w/ FBS, which uses the FBS technique to select 32 and 16 DCT coefficients for each color channel as input to the network, respectively.

The experiments were performed on a machine equipped with two 10-core Intel Xeon E5-2630v4 2.2 GHz processors, 64 GBytes of DDR4-memory, and 1 NVIDIA Titan Xp GPU. The machine runs Linux Mint 18.1 (kernel 4.4.0) and the ext4 file system. Fast-CoViAR was implemented in PyTorch (version 1.2.0) upon the CoViAR implementation<sup>4</sup>.

<sup>4</sup><https://github.com/chaoyuaw/pytorch-coviar> (As of October 2020)

Table 6 presents the classification accuracy achieved by Fast-CoViAR in each of the three splits of the UCF-101 and HMDB-51 datasets. We compare the results obtained by each stream in isolation and also for their combination. Among the different versions of ResNet-50 tested for the frequency stream, for the UCF-101 dataset, the one with the best performance was DCT, followed closely by DCT w/ FBS (32); while for the HMDB-51 dataset, the best was DCT w/ FBS (32) followed by DCT. This shows that the FBS technique is beneficial for the network, reducing its computational complexity without sacrificing accuracy. Notice that the frequency stream performs better than the temporal stream, however the results are improved when they are combined, showing that motion vectors from P-frames offer complementary information to DCT coefficients from I-frames. The best results were achieved by combining these two inputs, reaching classification accuracies of 86.0% on the UCF-101 dataset and 53.3% on the HMDB-51 dataset. These results indicate that the use of the information readily available in a compressed video is promising.

Table 7 compares the computational complexity and classification accuracy of Fast-CoViAR and CoViAR. Also, we considered the results reported by Wu et al. [12] for four baselines: ResNet-50 [30], ResNet-152 [30], C3D [31], and Res3D [32]. Similar to CoViAR [12], the computational costs for processing I-frames and P-frames are different and, for this reason, the values reported for Fast-CoViAR are the average GFLOPs over all frames. In terms of classification accuracy, Fast-CoViAR achieved the second best performance on the UCF-101 dataset and the third best performance on the HMDB-51 dataset. The highest classification accuracies were achieved by CoViAR. Since CoViAR and Fast-CoViAR use the same network for processing motion vectors from P-frames and the accuracy gains obtained by CoViAR with residuals from P-frames are marginal (less than 0.5%), we believe that it is because CoViAR processes information from I-frames using ResNet-152 [13], which is much deeper than ResNet-50 used by Fast-CoViAR. However, Fast-CoViAR has the smallest network computation complexity among all the baselines and is up to 2 times faster than CoViAR.

Table 8 compares the classification accuracy of Fast-CoViAR and the state-of-the-art compressed video methods. In general, Fast-CoViAR obtained comparable results on both the UCF-101 and HMDB-51 datasets, showing that it retains high accuracy while greatly reducing computational cost. Despite the results for EMV-CNN and DTMV-CNN were slightly better than Fast-CoViAR, in addition to motion vectors, they also use optical flow during the training phase. This feature can also be used by Fast-CoViAR, but its computation is significantly slower since video decoding is required.

The computational efficiency is the key advantage of Fast-CoViAR. To evaluate its efficiency, we measured the average inference time per-frame, which refers to the time spent for a forward pass through the network. For this, we sum up the total time taken to feed all the streams sequentially. To obtain a fair comparison, the forwarding time of CoViAR was measured using the authors' implementation, upon which we implemented Fast-CoViAR using the same code optimization.

Table 7: Comparison of the computation complexity (GFLOPs) and classification accuracy (%) of different networks. The best and the second best results are highlighted in bold and underlining, respectively.

Approach		GFLOPs	Accuracy (%)	
			<i>UCF-101</i>	<i>HMDB-51</i>
ResNet-50 [30]		3.8	82.3	48.9
ResNet-152 [30]		11.3	83.4	46.7
C3D [31]		38.5	82.3	51.6
Res3D [32]		19.3	85.8	<u>54.9</u>
CoViAR [12] <sup>5</sup>		4.2	<b>90.4</b>	<b>59.1</b>
Fast-CoViAR	DCT	2.7	85.7	53.3
	DCT w/ FBS (32)	<u>2.3</u>	<u>86.0</u>	52.7
	DCT w/ FBS (16)	<b>2.1</b>	84.7	52.1

<sup>5</sup>For a fair comparison, we considered the results reported by CoViAR [12] using only information from compressed domain. To improve its accuracy, CoViAR use optical flow besides motion vectors.

Table 8: Comparison of the classification accuracy (%) on the UCF-101 and HMDB-51 datasets for state-of-the-art compressed video based methods. The best and the second best results are highlighted in bold and underlining, respectively.

Approach		UCF-101	HMDB-51
EMV-CNN [10]		86.4	51.2 <sup>6</sup>
DTMV-CNN [11]		<u>87.5</u>	<u>55.3</u>
CoViAR [12]		<b>90.4</b>	<b>59.1</b>
Fast-CoViAR	DCT	85.7	53.3
	DCT w/ FBS(32)	86.0	52.7
	DCT w/ FBS(16)	84.7	52.1

<sup>6</sup>This result was reported in [11] and refers to the classification accuracy obtained only on Split 1 of the HMDB-51 dataset. We included here just for reference.

Figure 4 compares the classification accuracy, the network computation complexity, and the inference time for Fast-CoViAR and CoViAR on the UCF-101 and HMDB-51 datasets. Although CoViAR yields a higher classification accuracy, Fast-CoViAR leads to a significant speed-up, being around twice faster for inferences. Among the three variations of Fast-CoViAR, DCT w/ FBS (32) performs similar to or better than DCT, but is much more faster.



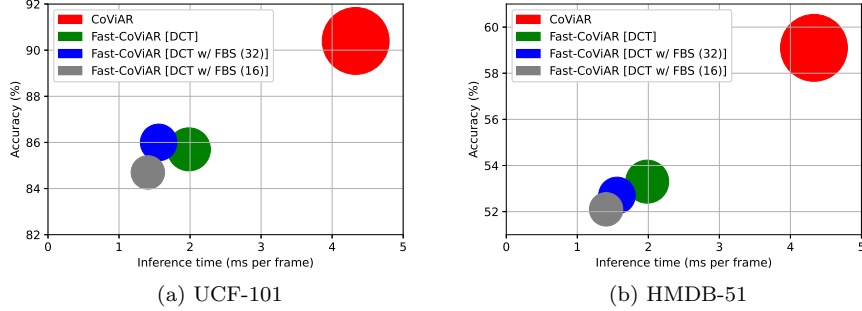


Figure 4: Comparison of the classification accuracy (%) and the inference time (ms per frame) for Fast-CoViAR and CoViAR on the UCF-101 and HMDB-51 datasets. Node size denotes the network computation complexity (GFLOPs).

## 6. Conclusion

In this paper, we presented a CNN designed to operate directly on frequency domain data, learning with DCT coefficients rather than RGB pixels. These information are readily available in the compressed representation of images and videos, saving the high computational load of fully decoding the data stream and greatly speeding up the processing time, which is currently a big bottleneck of deep learning. Our approach is an important step forward to make deep learning models more computationally efficient, enabling them to be used in devices with lower computational power and strict memory restrictions, for example, mobile phones and other edge devices.

The starting point of our proposal was the state-of-the-art model proposed by Gueguen et al. [9], which is a modified version of the ResNet-50 architecture [13]. Despite the speed-up obtained by partially decoding JPEG images, their architectural changes raised the computation complexity and the number of parameters of the network. To alleviate these drawbacks, we propose a Frequency Band Selection (FBS) technique to select the most relevant DCT coefficients before feeding them to the network.

For the task of image classification, we evaluated our approach on the ImageNet dataset. We analyzed the impact on computational complexity and accuracy of the network when only the 64, 32, and 16 lowest frequency DCT coefficients of each color component were selected to be used as input by our FBS method, where it proved to be effective in reducing the computational complexity of the network, while maintaining similar accuracy. We also evaluated the effects on the performance of CNNs fed with DCT coefficients under different spatial resolutions and JPEG quality settings. Our results demonstrated that the evaluated networks were robust to changes in the JPEG quality, but susceptible to variations in the spatial resolution.

In addition, we evaluated the performance of our model on the task of video classification on the UCF-101 and HMDB-51 datasets. To accomplish this, we

extended the CoViAR method [12] to have a frequency data stream with DCT coefficients as input to our modified ResNet-50 with FBS, instead of spatial stream with RGB pixels. Our network consists of a two-stream CNN integrating both frequency (i.e., transform coefficients) and temporal (i.e., motion vectors) information, whose predictions are combined by late fusion. The results we obtained demonstrated that the recognition performance of our network is similar to state-of-the-art methods, but its inference speed is up to 2 times faster. In short, our network is both faster and accurate.

As future work, we intend to evaluate smarter strategies for selecting DCT coefficients, like self-attention models. Also, we plan to extend our approach for video classification to use 3D network architectures, like Res3D [32] or I3D [33]. In addition, we want to evaluate smarter fusion strategies to combine the predictions of the two streams and to search for the optimal parameters of our network. Finally, we intend to evaluate our approach in large-scale datasets, like Kinetics [34], and in other applications.

## Acknowledgment

This research was supported by the FAPESP-Microsoft Research Virtual Institute (grant 2017/25908-6) and the Brazilian National Council for Scientific and Technological Development - CNPq (grants 423228/2016-1 and 313122/2017-2). We gratefully acknowledge the support of NVIDIA Corporation with the donation of the Titan Xp GPU used for this research.

## References

- [1] B. Deguerre, C. Chatelain, G. Gasso, Fast object detection in compressed JPEG images, in: IEEE Intelligent Transportation Systems Conference (ITSC'19), 2019, pp. 333–338.
- [2] Y. Li, S. Gu, L. V. Gool, R. Timofte, Learning filter basis for convolutional neural network compression, in: Proceedings of the IEEE International Conference on Computer Vision, 2019, pp. 5623–5632.
- [3] H. Li, A. Kadav, I. Durdanovic, H. Samet, H. P. Graf, Pruning filters for efficient convnets, arXiv preprint arXiv:1608.08710.
- [4] A. Marchisio, M. A. Hanif, F. Khalid, G. Plastiras, C. Kyrkou, T. Theocharides, M. Shafique, Deep learning for edge computing: Current trends, cross-layer optimizations, and open research challenges, in: IEEE Computer Society Annual Symposium on VLSI (ISVLS'19), 2019, pp. 553–559.
- [5] D. Xu, T. Li, Y. Li, X. Su, S. Tarkoma, P. Hui, A survey on edge intelligence, CoRR abs/2003.12172.

- [6] Z. Zhou, X. Chen, E. Li, L. Zeng, K. Luo, J. Zhang, Edge intelligence: Paving the last mile of artificial intelligence with edge computing, *Proceedings of the IEEE* 107 (8) (2019) 1738–1762.
- [7] G. Forecast, Cisco visual networking index: Global mobile data traffic forecast update 2017–2022, Update 2017 (2019) 2022.
- [8] M. Ehrlich, L. S. Davis, Deep residual learning in the JPEG transform domain, in: *IEEE International Conference on Computer Vision (ICCV’19)*, 2019, pp. 3484–3493.
- [9] L. Gueguen, A. Sergeev, B. Kadlec, R. Liu, J. Yosinski, Faster neural networks straight from JPEG, in: *Annual Conference on Neural Information Processing Systems (NIPS’18)*, 2018, pp. 3937–3948.
- [10] B. Zhang, L. Wang, Z. Wang, Y. Qiao, H. Wang, Real-time action recognition with enhanced motion vector cnns, in: *IEEE International Conference on Computer Vision and Pattern Recognition (CVPR’16)*, 2016, pp. 2718–2726.
- [11] B. Zhang, L. Wang, Z. Wang, Y. Qiao, H. Wang, Real-time action recognition with deeply transferred motion vector cnns, *IEEE Transactions on Image Processing* 27 (5) (2018) 2326–2339.
- [12] C.-Y. Wu, M. Zaheer, H. Hu, R. Manmatha, A. J. Smola, P. Krähenbühl, Compressed video action recognition, in: *IEEE International Conference on Computer Vision and Pattern Recognition (CVPR’18)*, 2018, pp. 6026–6035.
- [13] K. He, X. Zhang, S. Ren, J. Sun, Deep residual learning for image recognition, in: *IEEE International Conference on Computer Vision and Pattern Recognition (CVPR’16)*, 2016, pp. 770–778.
- [14] S. F. Santos, N. Sebe, J. Almeida, The good, the bad, and the ugly: Neural networks straight from jpeg, in: *IEEE International Conference on Image Processing (ICIP’20)*, 2020, pp. 1–5.
- [15] R. V. Babu, M. Tom, P. Wadekar, A survey on compressed domain video analysis techniques, *Multimedia Tools and Applications* 75 (2) (2016) 1043–1078.
- [16] S. F. Santos, N. Sebe, J. Almeida, CV-C3D: action recognition on compressed videos with convolutional 3d networks, in: *SIBGRAPI – Conference on Graphics, Patterns and Images (SIBGRAPI’19)*, 2019, pp. 24–30.
- [17] V. Bhaskaran, K. Konstantinides, *Image and Video Compression Standards: Algorithms and Architectures*, 2nd Edition, Kluwer Academic Publishers, Norwell, MA, USA, 1997.

- [18] K. Delac, M. Grgic, S. Grgic, Face recognition in JPEG and JPEG2000 compressed domain, *Image Vision Computing* 27 (8) (2009) 1108–1120.
- [19] P. Poursistani, H. Nezamabadi-pour, R. A. Moghadam, M. Saeed, Image indexing and retrieval in JPEG compressed domain based on vector quantization, *Mathematical and Computer Modelling* 57 (5-6) (2013) 1005–1017.
- [20] J. Almeida, N. J. Leite, R. S. Torres, Comparison of video sequences with histograms of motion patterns, in: *IEEE International Conference on Image Processing (ICIP’11)*, 2011, pp. 3673–3676.
- [21] W. Liu, D. Anguelov, D. Erhan, C. Szegedy, S. E. Reed, C.-Y. Fu, A. C. Berg, SSD: single shot multibox detector, in: *European Conference on Computer Vision (ECCV’16)*, 2016, pp. 21–37.
- [22] K. Simonyan, A. Zisserman, Two-stream convolutional networks for action recognition in videos, in: *Annual Conference on Neural Information Processing Systems (NIPS’14)*, 2014, pp. 568–576.
- [23] L. Wang, Y. Xiong, Z. Wang, Y. Qiao, D. Lin, X. Tang, L. V. Gool, Temporal segment networks: Towards good practices for deep action recognition, in: *European Conference on Computer Vision (ECCV’16)*, 2016, pp. 20–36.
- [24] L. Hanzo, P. Cherriman, J. Streit, *Video Compression and Communications: From Basics to H.261, H.263, H.264, MPEG4 for DVB and HSDPA-Style Adaptive Turbo-Transceivers*, 2nd Edition, John Wiley & Sons, Chichester, SXW, UK, 2007.
- [25] O. Russakovsky, J. Deng, H. Su, J. Krause, S. Satheesh, S. Ma, Z. Huang, A. Karpathy, A. Khosla, M. S. Bernstein, A. C. Berg, F.-F. Li, Imagenet large scale visual recognition challenge, *International Journal of Computer Vision* 115 (3) (2015) 211–252.
- [26] J. M. Chaquet, E. J. Carmona, A. Fernández-Caballero, A survey of video datasets for human action and activity recognition, *Computer Vision and Image Understanding* 117 (6) (2013) 633–659.
- [27] K. Soomro, A. R. Zamir, M. Shah, UCF101: A dataset of 101 human actions classes from videos in the wild, *CoRR* abs/1212.0402.
- [28] H. Kuehne, H. Jhuang, E. Garrote, T. A. Poggio, T. Serre, HMDB: A large video database for human motion recognition, in: *IEEE International Conference on Computer Vision (ICCV’11)*, 2011, pp. 2556–2563.
- [29] D. P. Kingma, J. Ba, Adam: A method for stochastic optimization, *CoRR* abs/1412.6980.
- [30] C. Feichtenhofer, A. Pinz, R. P. Wildes, Spatiotemporal multiplier networks for video action recognition, in: *IEEE International Conference on Computer Vision and Pattern Recognition (CVPR’17)*, 2017, pp. 7445–7454.

- [31] D. Tran, L. D. Bourdev, R. Fergus, L. Torresani, M. Paluri, Learning spatiotemporal features with 3d convolutional networks, in: IEEE International Conference on Computer Vision (ICCV'15), 2015, pp. 4489–4497.
- [32] D. Tran, J. Ray, Z. Shou, S.-F. Chang, M. Paluri, Convnet architecture search for spatiotemporal feature learning, CoRR abs/1708.05038.
- [33] J. Carreira, A. Zisserman, Quo vadis, action recognition? A new model and the kinetics dataset, in: IEEE International Conference on Computer Vision and Pattern Recognition (CVPR'17), 2017, pp. 4724–4733.
- [34] W. Kay, J. Carreira, K. Simonyan, B. Zhang, C. Hillier, S. Vijayanarasimhan, F. Viola, T. Green, T. Back, P. Natsev, M. Suleyman, A. Zisserman, The kinetics human action video dataset, CoRR abs/1705.06950.